Semnan University

Progress in Physics of Applied Materials

journal homepage: https://ppam.semnan.ac.ir/

Effect of Aluminum Doping on the Optical, Electrical, and Gas Sensing Properties of ZnO Thin Films

Samundra Marasini [a,*], Sumitra Pandey [a], Rishi Ram Ghimire [b], Pramod Subedi [c]

[a]*Goldengate International College, Tribhuvan University, Kathmandu, Nepal*
[b]*Department of Physics, Patan Multiple Campus, Tribhuvan University, Patandhoka, Lalitpur, Nepal*
[c]*Physical Science Laboratory, Nepal Academy of Science and Technology, Lalitpur, Nepal*

ARTICLE INFO

Article history:
Received: 20 September 2024
Revised: 29 October 2024
Accepted: 30 October 2024

Keywords:

Aluminum doping
ZnO thin films
Optical properties
Electrical properties
Blood serum

ABSTRACT

The study explored the effects of aluminum doping on the optical and electrical properties of ZnO thin films, along with their gas sensing capabilities, specifically in response to blood serum. ZnO thin films were prepared using a spin-coating method, followed by annealing at 500°C, with varying Al doping concentrations (0%, 0.5%, 1%, 1.5%, 2%, and 2.5%). The results showed that higher Al doping concentration improved the transmittance by 85%, likely due to enhanced crystallinity and the Burstein-Moss effect. The refractive index and extinction coefficient analyses indicated a decrease in light absorption and scattering at higher doping levels, reflecting improved film quality. The real and imaginary parts of the dielectric constant also varied with doping, with 0.5% Al-doped ZnO showing the highest real part, suggesting better dielectric properties. The optical band gap of Al-doped ZnO films decreased with increasing Al concentration, consistent with previous studies, indicating potential improvements in electrical conductivity. The electrical properties, particularly I-V characteristics, revealed that higher Al doping decreased conductivity, likely due to increased charge carrier scattering. Gas sensing experiments demonstrated that 2% Al-doped ZnO exhibited higher sensitivity to blood serum, while resistance varied with time and serum volume, highlighting the dynamic interaction between the ZnO films and their environment. The study's findings suggest that Al doping enhances the optical and sensing properties of ZnO thin films, with an optimal doping concentration around 2% for maximum sensitivity.

1. Introduction

The main driving force behind ZnO research is its significant potential for diverse practical applications, including use in optoelectronic devices like sunscreens, LCDs, LEDs, laser diodes, photodetectors, solar cells, energy harvesting devices, transistors, sensors, catalysts, and active sunscreen compounds [1, 3]. ZnO is also valued for its high electrochemical and thermal stability, as well as its role as an air-stable anode in organic LEDs [4, 5]. The wide range of synthesis techniques and nanostructures, combined with excellent characterization properties, further increases its demand. Among the many deposition techniques, spin coating is particularly preferred for thin film deposition on flat substrates due to its cost-effectiveness, ease of doping, and control over spin and film thickness. This technique's success suggests that ZnO-based films could potentially rival and replace the longstanding dominance of indium tin oxide (ITO) or ITO-based systems, which rely on the more expensive and less abundant indium [6]. In this research, aluminum-doped zinc oxide (AZO) films were utilized to fabricate a blood serum sensor, an important tool for disease diagnosis.

* Corresponding author. Tel.: +977 984-1091121
E-mail address: samundramarasini.sm@gmail.com

Cite this article as:
Marasini, S., Pandey, S., Ghimire, R., Subedi, P, 2025. Effect of Aluminum Doping on the Optical, Electrical, and Gas Sensing Properties of ZnO Thin Films. *Progress in Physics of Applied Materials*, *5*(1), pp.1-9.DOI: 10.22075/ppam.2024.35384.1118

ZnO, known for its versatility and early discovery, is also a widely used material in gas sensing due to its stability and broad sensitivity range. The material's optical properties involve the excitation of charge carriers from the valence band to the conduction band, leading to increased conductivity through the desorption of surface oxygen by photogenerated holes. ZnO exhibits both direct and indirect optical absorption, with direct absorption involving photon absorption and the creation of electron-hole pairs, while indirect absorption separates electrons and holes by the minimum energy of the band structure. Defect states within the band gap region are crucial for optical absorption and emission in ZnO [7].

Jantrasee et al., explored the impact of Al concentration on the structural and optical properties of Al-doped ZnO thin films, examining optical parameters such as band gap, dispersion parameters, refractive index, absorption coefficient, and optical conductivity [8]. Al incorporation influenced dispersion energy, average oscillator wavelength and strength, single oscillator energy, and refractive index. ZnO nanomaterials exhibit various structures ranging from zero-dimensional (nanoparticles) to three-dimensional forms, including nanorods, nanosheets, and hierarchical films. One-dimensional ZnO structures like nanotubes [9] and nanowires [10] correspond to linear geometries, while two-dimensional nanodisks [11] result from lateral crystal growth.

The study conducted by Eisa and Faraj [12] compared the properties of thin films made from aluminum-doped zinc oxide (AZO), gallium-doped zinc oxide (GZO), and indium-doped tin oxide (ITO), all of which were deposited using radio-frequency magnetron sputtering. Their findings showed that reducing the energy of oxygen-negative ions during the deposition process notably enhanced the uniformity and reduced the resistivity of AZO thin films. This improvement was observed specifically in AZO films, highlighting the distinct advantages of aluminum doping in zinc oxide thin films over other doped variants. In a related study [13], the effects of varying aluminum doping ratios on AZO films created through mist chemical vapor deposition were explored. The research demonstrated that different Al/Zn ratios had a significant impact on the films' structural and optical characteristics. AZO films with aluminum doping concentrations between 1 wt% and 3 wt% maintained high optical transmittance (>80%) within the visible spectrum. The film with 2 wt% aluminum showed the highest photocatalytic activity under UV light, underscoring the suitability of AZO films for photocatalytic and biosensing applications.

The p-n heterostructures, specifically CeO_2 configurations, optimized for photodetection, featuring tunable CeO_2 concentrations. Through hydrothermal and sputtering methods, this ternary structure displays enhanced UV photodetection performance, rapid response/decay times, and consistent current under UV light, especially with 5.5% CeO_2 [14]. ZnO, recognized for its wide bandgap, is pivotal in UV detection for fields like space and radiation monitoring. Ce doping enhances UV sensitivity under laser excitation, yielding a higher detectivity and efficient response [15]. ZnO's gas sensitivity, particularly for CO, improves via sputtered Al-doped films, as deposition parameters optimize porosity and response values [16]. Additional studies show Al-doped ZnO thin films enhance conductivity, optical properties, and potential in solar cells and UV photodetectors [17, 18]. Co-doping ZnO with Al and Cu shows high transparency, desirable for optoelectronics. Co-doped samples balance optical bandgap and carrier density for improved conductivity [19]. Further, Al-doped ZnO nanostructures, fabricated through chemical vapor deposition, show increased photocatalytic efficiency and enhanced optoelectronic properties with Al levels up to 0.08, beneficial for multiple applications [20].

The novelty of this research lies in its unique exploration of aluminum-doped ZnO thin films for gas sensing applications using blood serum, which has not been previously studied. While past research has focused on doping effects on optical and electrical properties, no work has addressed the interaction of such films with blood serum. This study not only demonstrates enhanced optical properties and sensitivity with Al doping but also reveals a novel application in biomedical sensing, making it distinct from prior investigations.

2. Materials and Methods

2.1. Sample preparation

Glass slides were cut into 2.5 cm x 2.5 cm pieces, cleaned with dilute HCl, rinsed with distilled water, boiled in acetone at 70°C, and then dried. A precursor solution was created by dissolving 2.74 g of zinc acetate in 25 ml of propanol, stirring it at 60°C for 30 minutes, and gradually adding diethylamine until a clear solution formed, which was then left to stand for 24 hours. For doping, varying concentrations (0%, 0.5%, 1%, 1.5%, 2%, and 2.5%) of aluminum chloride hexahydrate were dissolved in a mixture of propanol and distilled water and combined with 25 ml of the zinc acetate solution. Thin films were then produced by applying 0.1 ml of both undoped and Al-doped solutions onto a spinning substrate using a spin-coater, followed by annealing at 500°C for 15 minutes. This process was repeated up to 12 times until the film's resistance decreased to a few hundred kiloohms, making them suitable for application.

2.2. Characterization of Thin Film

The optical properties of the Al- -doped ZnO thin films were assessed using UV-Vis spectrophotometry with a Carry 60 spectrophotometer. This method enabled the examination of absorbance and transmittance spectra, offering valuable data on the films' optical band gap and transparency.

2.3. Experimental setup

The gas sensing device consisted of an airtight wooden chamber equipped with separate inlet and outlet openings, along with a heating element. The resistance of the ZnO films was monitored before and after exposure to blood serum at temperatures of 60°C, 80°C, and 100°C. The temperature of the heater was adjusted using a variable voltage regulator and a rheostat. Sensitivity was calculated as the ratio of the resistance change in the presence of gas to the resistance in air. The films were cut, heated, and connected with silver paste to create sensors, which were then placed in a cubic wooden box with openings for serum injection and wire connections. The sensors were tested using serum volumes of 25 µL, 50 µL, 75 µL, and 100 µL at various temperatures. The detail visualization of sketch and real experimental setup is shown in Fig. 1.

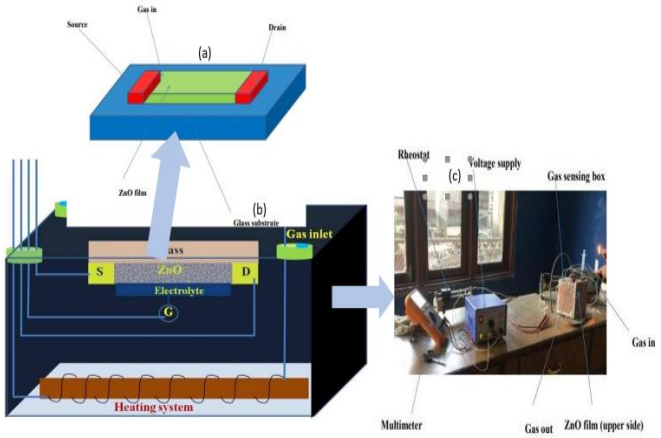

Fig. 1: Sensing measurement setup (a) Designed diagram, (b) Sensor and (c) real system.

2.4. Gas Sensing Mechanism

The gas sensing mechanism is primarily based on electron transfer between absorbed oxygen species and the molecules of the test gas. The sensor's response is largely influenced by the quantity of absorbed oxygen species, as well as the specific surface area, structure, active sites, and electron characteristics of the sensing material. The detection of gas is accomplished by observing changes in the sensor's resistance.

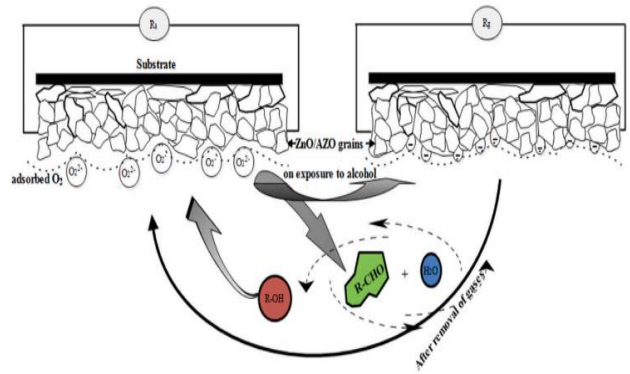

Fig. 2: Sensing Mechanism of ZnO/AZO thin Film.

The gas sensing mechanism of Metal Oxide (MOx) semiconductors is shown in fig. 2, which is relevant in this experiment, typically involves the adsorption of atmospheric oxygen on the oxide surface. This process extracts electrons from the semiconductor, resulting in changes in carrier density and conductivity. The interaction with oxidizing or reducing gases alters the oxygen concentration and conductivity, enabling the measurement of gas concentration. The effects of oxidizing and reducing gases are opposite to each other.

3. Results and Discussion

The study evaluated the optical properties (transmittance, refractive index, extinction coefficient, dielectric properties, and band gap) and electrical properties (I-V characteristics, resistance vs. time) of lab-designed ZnO thin films. It also analyzed the sensor's response and sensitivity to blood serum across different doping concentrations and temperature ranges.

3.1. Optical Properties of Al dopped ZnO

The findings presented in Fig. 3 highlight the influence of aluminum doping on the transmittance properties of ZnO thin films. Specifically, the 2.5% Al-doped ZnO film exhibited a high transmittance value of approximately 85%, suggesting enhanced crystallinity and making it a suitable candidate for use as solar cell electrodes. This high transmittance indicates that the film allows a significant amount of light to pass through, which is crucial for efficient solar energy conversion. The low doping concentration (0.5% Al), the less aluminum atoms are incorporated into the ZnO lattice, meaning that their concentration is not high enough to significantly enhance the crystallinity of the material. The presence of fewer Al atoms may not fully passivate defect sites, leading to more scattering centers within the film. These scattering centers can trap light, reducing the overall transmittance. This explains why the 0.5% Al-doped ZnO film showed lower transmittance (starting around 35% and increasing to 47%) compared to films with higher doping levels. The higher doping concentration (2.5% Al), the more Al atoms substitute for Zn in the lattice. This substitution can lead to a reduction in oxygen vacancies and other defects, resulting in improved crystalline quality. A better-ordered crystal structure scatters less light and allows lighter to pass through the film, thereby increasing transmittance. The 2.5% Al-doped ZnO film exhibited a transmittance of approximately 85%, indicating that higher doping enhances crystallinity and reduces light scattering. The transmittance nature with wavelength was found similar to [21] with concentration of 0.5 % to 3%.

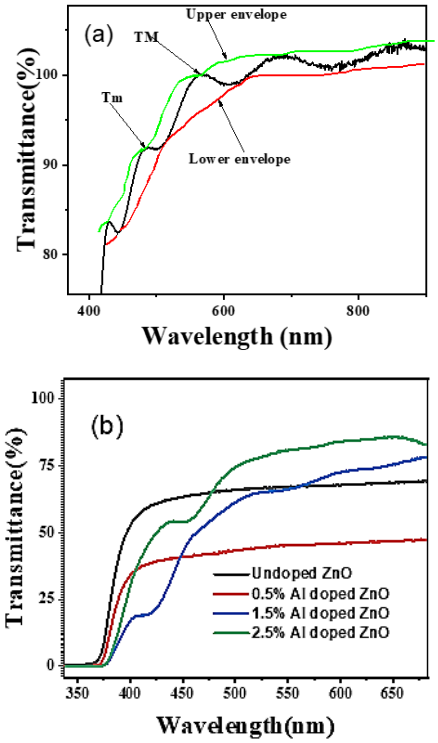

Fig. 3:(a) Transmittance of 2.5% Al doped ZnO, and (b)transmittance of undoped, and 0.5%, 1.5%, 2.5% Al doped ZnO.

The increase in transmittance with higher Al doping can also be attributed to the Burstein-Moss effect. Doping with aluminum introduces additional free electrons into the conduction band of ZnO, leading to a shift in the Fermi level into the conduction band. This results in a widening of the optical bandgap, known as a "blue shift," because higher-energy photons (in the UV region) are now required to excite electrons across the bandgap. Consequently, the material becomes more transparent to visible light, enhancing transmittance. In comparison to the findings Zhu et al., where a 3.0% Al doping led to a decrease in transmittance, the current study observed an increase in transmittance with Al doping up to 2.5%. This discrepancy may be explained by differences in film deposition techniques, thicknesses, or post-deposition annealing processes, which can affect the distribution and incorporation of Al atoms in the ZnO lattice. If doping concentrations exceed an optimal level, it could lead to the formation of secondary phases or an increase in scattering centers, which would reduce transmittance, as observed in Zhu et al.'s study [22].

The refractive index of the film was calculated by using Fresnel's equation (1) as

$$n = \frac{1+R}{1-R} + \sqrt{\frac{4R}{(1-R)^2} - k^2} \qquad (1)$$

where, n is the refractive index, R is reflectance (it is measured using UV spectrometer directly) and k is extinction coefficient also given by equation (2)

$$k = \frac{\lambda a}{4\pi} \qquad (2)$$

where a is absorbance. The analysis of refractive index and extinction coefficient variations with wavelength, as illustrated in Fig. 4(a) and Fig. 4(b), provides insights into the optical behavior of aluminum-doped ZnO thin films across the wavelength range of 400 nm to 800 nm.

Refractive index analysis [Fig. 4(a)] shows the refractive index of 0.5% Al-doped ZnO decreases exponentially from approximately 2.25 at 300 nm to 1.5 at 400 nm. This decrease continues into the visible region, reaching a lower value at 800 nm. The exponential decrease in the refractive index with increasing wavelength suggests that the film's ability to bend light diminishes as the wavelength increases. Also, for 1.5% and 2.5% Al-doped ZnO, the refractive index exhibits a similar trend but starts from a lower initial value and decreases more gradually. The refractive index for these samples is lower compared to the 0.5% Al-doped ZnO, and the rate of decrease with wavelength is less pronounced. The decrease in refractive index with increasing wavelength is attributed to reduced absorbance and scattering of light within the film. As the aluminum doping concentration increases, the ZnO film's structural quality improves, which reduces the number of defects and scattering centers that would otherwise interact with light. This reduction in scattering contributes to a lower refractive index, especially noticeable in the visible spectrum. The nature of refractive index as shown in fig. 4 found similar to Baydogan et al. report [23]. Generally, the refractive index has shown decrement with wavelength increment, [16-23]. Also, the extinction coefficient has similar nature for undoped and lower Al dopped ZnO as observed in Fig. 4(b).

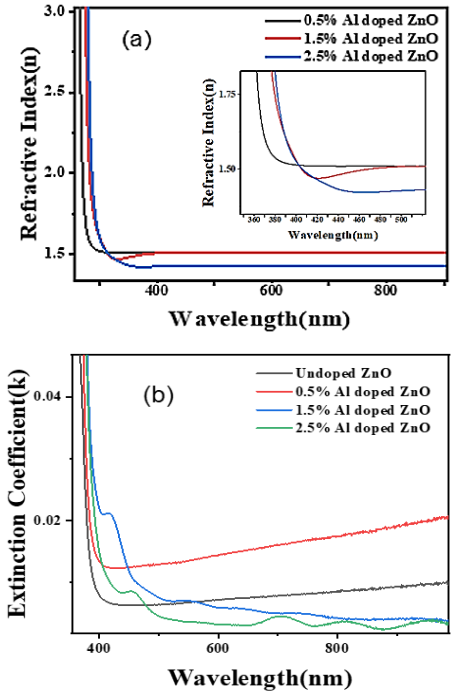

Fig. 4: Refractive Index (a), and extinction coefficient of undoped (b) of undoped, 0.5%, 1.5%, and 2.5% Al doped ZnO vs wavelength.

Extinction coefficient analysis [Fig. 4(b)] indicates that the extinction coefficient (k) is higher for the 0.5% Al-doped ZnO sample than that for the other samples. This higher value indicates greater absorption of light within this film, likely due to the presence of more defect states or lower crystallinity, which increases the material's ability to absorb light. For 2.5% Al-doped ZnO: Conversely, the extinction coefficient is lower for the 2.5% Al-doped ZnO film. The decrease in k suggests that higher doping

concentrations improve the film's crystalline quality, thereby reducing light absorption due to fewer defect states and less scattering. The extinction coefficient is directly related to the material's absorption of light. A higher extinction coefficient at lower doping concentrations indicates more significant absorption due to the increased presence of defect states and reduced crystallinity. In contrast, the lower extinction coefficient for higher doping levels reflects improved film quality and fewer absorption centers. Higher Al doping enhances the film's transparency by reducing absorption and scattering, which is reflected in the reduced extinction coefficient. Also, the nature of refraction index changes with wavelength in the present study is similar to Zhai et al.'s report [24] while the extinction coefficient changes with respect to wavelength is quite different from what they found.

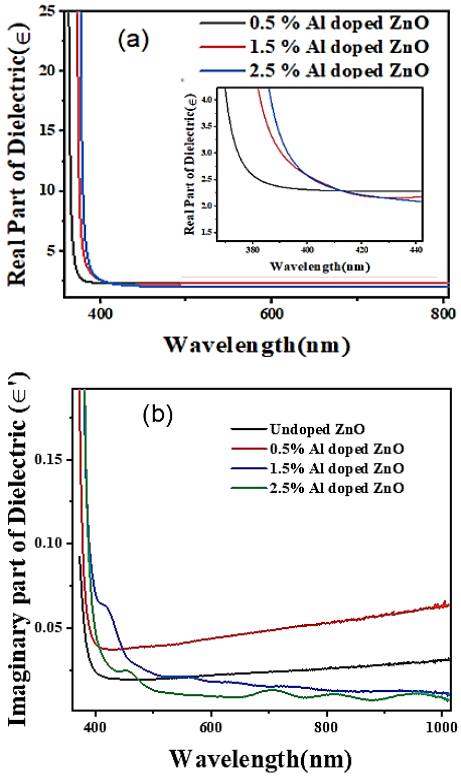

Fig. 5: Dielectric constants, (a) real part, and (b) imaginary part, vs wavelength of undoped and doped ZnO films.

The real and imaginary parts of dielectric constant were obtained using analytical method using following formula [25],

$$\in(w) = \epsilon + i\,\epsilon' \qquad (3)$$

where ϵ is real and ϵ' is imaginary part of the complex dielectric function encloses the desired information of nanostructured thin film $\epsilon = n^2 - k^2$ and $\epsilon' = 2nk$. The real and imaginary parts are distinctly related to refractive index (n) and extinction coefficient (k). Fig. 5(a) and 5(b), reveal important trends in their optical behavior. The real part of the dielectric constant (ϵ) is notably higher than the imaginary part (ϵ') across all doping concentrations, indicating that the films have strong dielectric storage capabilities [26]. Among the samples, the 0.5% Al-doped ZnO film exhibits the highest real part, suggesting it possesses superior dielectric properties and potentially better transparency. However, as the doping concentration increases to 1%, 1.5%, and 2.5%, the real part of ϵ decreases, which could be due to changes in the film's structure or increased defect densities. In contrast, the imaginary part of the dielectric constant, representing dielectric losses or absorption, is lower than the real part for all doping levels, reflecting that the films generally have good transparency and low dielectric losses. The 0.5% Al-doped ZnO sample also shows the highest imaginary part, indicating higher absorption losses compared to films with higher doping concentrations. The decrease in ϵ" with increased doping concentration implies improved transparency and reduced dielectric losses in these films. Additionally, the measurement of the real part of the dielectric constant was only successful for three doping concentrations, suggesting potential issues with noises or disturbances in the data for one sample. This highlights the need for careful sample preparation and accurate measurement techniques to ensure reliable results. Overall, the findings suggest that while the 0.5% Al-doped ZnO films offer a favorable balance of high dielectric constant and good transparency, higher doping levels can enhance transparency but may alter dielectric properties and introduce measurement challenges.

3.2. Optical band gap of Al dopped ZnO

It has been observed that the direct optical bandgap of Al-doped ZnO films exhibits a decreasing trend with increasing Al concentration, as depicted in Fig. 6. Specifically, the bandgap for undoped ZnO is 3.25 eV, while for 0.5% Al-doped ZnO, it increases slightly to 3.35 eV. However, further doping reduces the bandgap, with both 1.5% and 2.5% Al-doped ZnO showing an optical bandgap of 3.20 eV. These findings are consistent with previous research by Jantrasee et al. [8] and Shirouzu et al. [27], where the optical bandgap of ZnO was reported as 3.15 eV, and the optical band gaps of Al-doped ZnO were found to decrease progressively from 3.07 eV to 2.95 eV with increasing Al doping. This happened because the energy required for electrons to jump from the valence band to the conduction band (the bandgap) decreases. Initially, the bandgap of pure ZnO is 3.07 eV, but as the concentration of Al increases, the bandgap reduces to 2.95 eV. This reduction occurs because aluminum doping introduces additional free electrons and modifies the electronic structure of ZnO, causing a narrowing of the bandgap, which affects the material's optical and electrical properties.

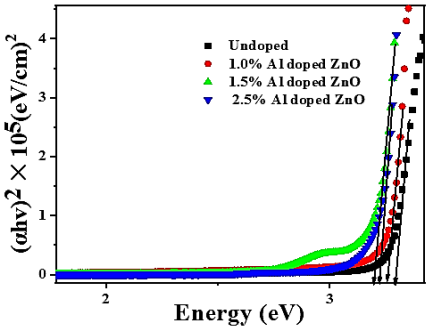

Fig. 6: Comparison of optical band gaps of undoped, 0.5%, 1.5% and 2.5% Al- Doped ZnO

This redshift in the bandgap upon incorporating Al into ZnO is primarily attributed to the active transitions involving 3d

levels in Al^{3+} ions and the strong sp-d exchange interaction between the traveling "sp" carriers (band electrons) and the localized "d" electrons of the dopant. The narrowing of optical band gap not only aligns with these studies but also suggests potential improvements in electrical conductivity, as a reduced bandgap facilitates easier electron transitions, thereby enhancing the material's conductive properties. This effect is crucial for applications where increased electrical conductivity is desirable, such as in optoelectronic devices.

Fig. 7 illustrates the relationship between the optical band gap and varying Al doping concentrations. The graph reveals a linear decrease in the optical band gap as the Al concentration increases, indicating a direct correlation between the two. This linear trend continues up to a certain maximum doping limit, beyond which the quenching of the optical band gap stabilizes, suggesting that further increases in Al concentration may not significantly impact the optical band gap. This behavior highlights the importance of optimizing the doping level to achieve desired electronic properties without compromising material performance.

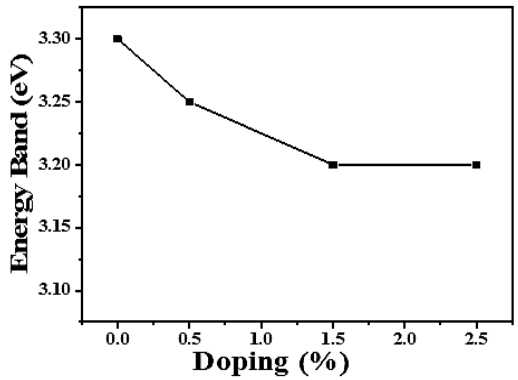

Fig. 7: Optical Band gap Vs Al doping concentration of ZnO films.

3.3. *Electrical Properties, Sensitivity, Response with serum*

The significance of the electrical properties of ZnO films, particularly the relationship between voltage and current, is illustrated through the I-V curve in Fig. 8(a). As the voltage increases, the current also increases, demonstrating a linear behavior. The undoped ZnO film shows a relatively high current of approximately 431 µA at high voltage, likely due to differences in sample size dimensions. In contrast, the ZnO film doped with 2.5% Al exhibits a much smaller increase in current, reaching only 17 µA. This reduction in current with higher Al concentration suggests that Al doping decreases the film's conductivity, which may be due to the increased scattering of charge carriers or changes in the film's crystalline structure.

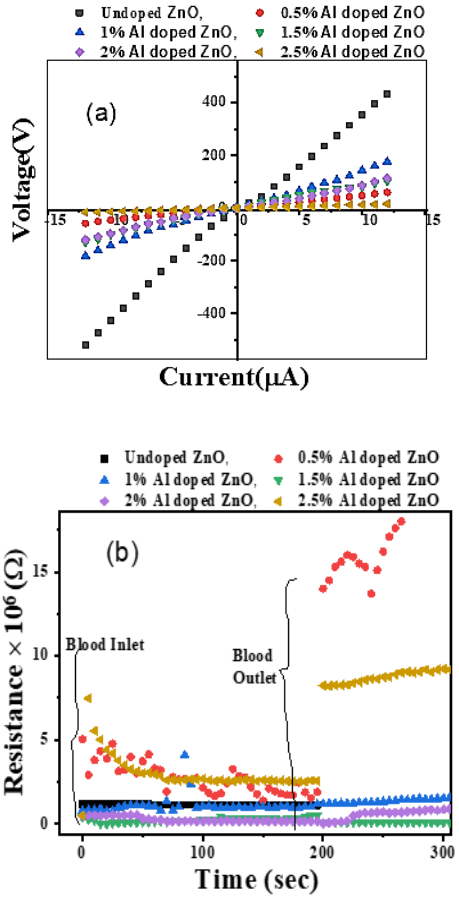

Fig. 8: IV characteristics (a) voltage vs current, and (b) resistance time at undoped, 0.5%, 1%, 1.5%, 2% and 2.5% Al doped ZnO at 80°C with 100 µl serum

Figure 8(b) presents the resistance of ZnO films with time for different Al dopant concentrations. When gas (in this case, blood serum) is introduced, the resistance decreases initially for a few seconds and then remains constant for about 100-130 seconds. After this period, the resistance begins to rise, eventually returning to or even exceeding its original value within the next 100 seconds. This behavior is consistent with the findings [28], who observed similar transfer characteristics in ZnO and Al-doped ZnO (AZO) channels in EDL-gated TFTs. The initial decrease in resistance could be due to the adsorption of gas molecules on the film's surface, which facilitates charge carrier movement. As the gas is desorbed or reacts with the surface, the resistance increases, restoring the film to its original state. The variation in resistance over time highlights the dynamic interaction between the ZnO film and the surrounding environment, which is influenced by Al doping levels.

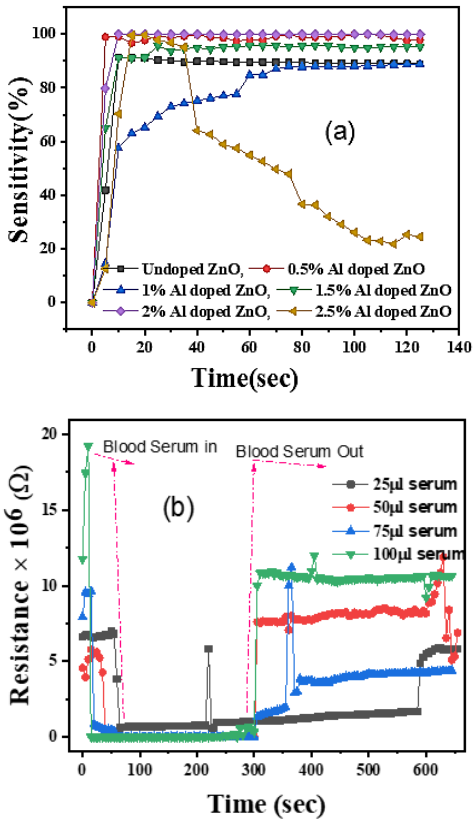

Fig. 9: Nature of (a) sensitivity of undoped ZnO and doped with Al of different concentrations to 25 µl serum, and (b) resistance of undoped ZnO with time for ~~of~~ 25 µl, 50 µl, 75 µl, and 100 µl blood serum at 60 °C

Fig. 9(a) represents the sensitivity of undoped ZnO and doped with Al of different concentrations to 25 µl serum. From the observations in Fig. 9(a), it is evident that 2% Al-doped ZnO maintains consistently higher sensitivity compared to other doping concentrations. Notably, 2.5% Al-doped ZnO initially exhibits similar sensitivity levels within the first 40 seconds but does not sustain this over time. In contrast, 1% Al-doped ZnO shows lower sensitivity throughout the experiment. This suggests that as the concentration of Al doping increases, the sensitivity of the ZnO film generally improves, likely due to enhanced surface reactivity and charge carrier dynamics. However, the optimal doping concentration appears to be around 2%, beyond which the benefits may diminish or plateau. The higher sensitivity of 2% Al-doped ZnO, as observed in the experiment, is likely due to enhanced surface reactivity and optimal charge carrier dynamics at this concentration. Al doping increases the number of active sites on the ZnO surface, facilitating better interaction with the gas molecules (in this case, blood serum). This improves gas adsorption and desorption processes, leading to a more efficient sensing response. This behavior indicates that there is an optimal doping level (around 2%) where the balance between enhanced surface reactivity and minimal charge carrier scattering results in the highest sensitivity.

In addition, Fig. 9(b) illustrates the resistance behavior of ZnO films over time when exposed to different volumes of blood serum. Initially, there is a noticeable decline in resistance as the blood serum interacts with the sensing device. This drop in resistance during the initial time intervals could be due to the adsorption of biomolecules from the serum onto the ZnO surface, which facilitates charge transfer and reduces resistance. The resistance then stabilizes and remains steady until approximately 250 seconds, after which it begins to increase as the gas is passed out of the system. This increase in resistance could indicate desorption of the serum or a reduction in the availability of charge carriers as the interaction between the serum and the ZnO surface diminishes. These observations underscore the dynamic and time-dependent nature of the sensing mechanism, where the optimal sensitivity and resistance response are influenced by both Al doping concentration and the interaction with the blood serum.

In Fig. 10(a), the sensitivity of undoped ZnO and doped with Al of different concentrations at 60°C to 25 µl blood serum is analyzed. The sensitivity across all blood serum concentrations initially rises for the first 40 seconds, indicating an active interaction between the serum and the sensing material. After this initial increase, the sensitivity stabilizes, maintaining a constant level for the majority of the observed time period, which spans approximately 200 seconds. This stability suggests that the sensor reaches a saturation point where the interaction between the blood serum and the ZnO film remains consistent. Although not shown in the graph, it is noted that sensitivity eventually begins to decrease after this period, likely due to desorption processes or a reduction in active binding sites on the ZnO surface. Blood serum is used because it contains a range of biomolecules, including proteins and enzymes, which can interact with specific gases or volatile organic compounds (VOCs). These interactions can be detected and measured using biosensors. In particular, hemoglobin and other blood components can bind to gases like oxygen, carbon dioxide, and carbon monoxide, making blood a potential medium for detecting gas concentrations.

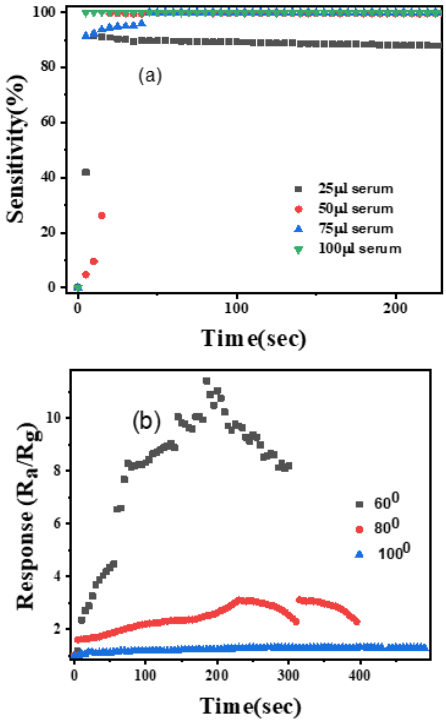

Fig. 10: Sensitivity of (a) undoped and Al-doped ZnO at 60°C, and (b) response at different temperature with 1% Al doped ZnO and 25 µl blood serum

Fig. 10(b) focuses on the response of 1% Al-doped ZnO to 25 µl blood serum at the same temperatures. At 60°C, the ZnO film demonstrates a strong response to serum sensing, with the sensitivity rapidly increasing in the first few seconds and reaching a peak value of nearly 12. However, after reaching this peak, the response begins to decline, indicating that the sensor has reached its maximum sensitivity at this temperature and is now experiencing a reduction in active interaction. In contrast, at 80°C and 100°C, the response of the 1% Al-doped ZnO is significantly lower. This suggests that 60°C is the optimal temperature for serum sensing with this specific doping concentration, as higher temperatures may lead to faster desorption or degradation of the serum-ZnO interaction, resulting in reduced sensitivity.

4. Conclusion

This study provides a comprehensive analysis of aluminum-doped zinc oxide (ZnO) thin films, focusing on their optical, electrical, and gas-sensing properties. The optical analysis revealed that higher aluminum doping levels enhance the transmittance of ZnO films, with 2.5% Al-doped ZnO exhibiting the highest transmittance of approximately 85%. The refractive index and extinction coefficient analysis further confirmed that higher doping levels reduce light scattering and absorption, resulting in superior optical properties. The electrical characterization indicated that aluminum doping decreases the conductivity of ZnO thin films. The I-V measurements showed that undoped ZnO films exhibit higher currents compared to Al-doped films, with the 2.5% Al-doped ZnO displaying the lowest current values. The gas sensing experiments demonstrated that the sensitivity of ZnO thin films to blood serum varies with aluminum doping concentration and temperature. Notably, 2% Al-doped ZnO films exhibited consistently higher sensitivity, suggesting an optimal doping concentration for gas sensing applications.

Conflicts of Interest

The authors declare that there is no conflict of interest regarding the publication of this article.

References

[1] Dhale, B. B., Mujawar, S. H., Bhattar, S. L., and Patil, P. S., 2014. Chemical properties of n-ZnO/p-CuO heterojunctions for photovoltaic applications. Der Chemica Sinica, 5(4), pp. 59-64.

[2] Klingshirn, C.F., Meyer, B.K., Waag, A., Hoffmann, A., and Geurts, J., 2010. Zinc Oxide: From Fundamental Properties towards Novel Applications. Springer, New York.

[3] Yan, H., He, R., Pham, J., and Yang, P., 2003. Morphogenesis of one-dimensional ZnO nano- and microcrystals. Advanced Materials, 15, pp. 402-405.

[4] Dang, W. L., Fu, Y. Q., Luo, J. K., Flewitt, A. J., and Milne, W. I., 2007. Deposition and characterization of sputtered ZnO films. Superlattices and Microstructures, 42, pp. 89-93.

[5] Yun, S. N., Lee, J. Y., Yang, J. Y., and Lim, S. W., 2010. Hydrothermal synthesis of Al-doped ZnO nanorod arrays on Si substrate. Physica B, 405, pp. 413-419.

[6] Rwenyagila, E. R., Tuffor, B. A., Z-Kana, M. G., Kin-Ojo, O. A., and Soboyeja, W. O., 2014. Optical properties of ZnO/Al/ZnO multilayer films for large area transparent electrodes. Journal of Materials Research, 29(24), pp. 28-38.

[7] Viezbicke, B. D., Patel, S., Davis, B. E., and Birnie, D. P., III, 2015. Physica Status Solidi (b), 252, p.p. 1700-1710.

[8] Jantrasee, S., Moontragoon, P., and Pinitsoontorn, S., 2016. Thermoelectric properties of Al-doped ZnO: experiment and simulation. Journal of Semiconductors, 37(9), 092002.

[9] Zhou, F., Jing, W., Liu, P., Han, D., Jiang, Z., and Wei, Z., 2017. Doping Ag in ZnO nanorods to improve the performance of related enzymatic glucose sensors. Sensors, 17, 2214.

[10] Wang, H. H., Chen, X. J., Li, W. T., Zhou, W. H., Guo, X. C., Kang, W. Y., Kou, D. X., Zhou, Z. J., Meng, Y. N., and Tian, Q. W., 2018. ZnO nanotubes supported molecularly imprinted polymers arrays as sensing materials for electrochemical detection of dopamine. Talanta, 176, pp. 573-581.

[11] Aydin, C., 2019. Synthesis of Pd: ZnO nanofibers and their optical characterization dependent on modified morphological properties. Journal of Alloys and Compounds, 777, pp. 145-151.

[12] Eisa, M. H., and Faraj, M. G., 2022. Optical properties of Al-doped ZnO (AZO) thin films with PLD technique. Digest Journal of Nanomaterials and Biostructures.

[13] Li, Y., Liu, X., Wen, D., Lv, K., Zhou, G., Zhao, Y., Xu, C., and Wang, J., 2020. Growth of c-plane and m-plane aluminium-doped zinc oxide thin films: epitaxy on flexible substrates with cubic-structure seeds. Acta Crystallographica Section B: Structural Science, Crystal Engineering and Materials, 76(Pt 2), pp. 233-240.

[14] Banari, M., Memarian, N., Concina, I., and Vomiero, A., 2023. UV photodetector study based on Ce: ZnO nanostructures with different concentrations of Ce dopant. Optical Materials, 146, p. 114576.

[15] Banari, M., Memarian, N., Kumar, P., You, S., Vomiero, A., and Concina, I., 2024. CeO_2: ZnO hybrid nanorods for self-powered UV-photodetectors. Ceramics International.

[16] Hu, S. H., Lin, Y. S., Su, S. H., He, J. S., and Ai, Y. Z., 2024. Improving surface structures of Al-doped zinc oxide thin films to apply in CO gas-sensing property by designing processes through RF magnetron sputtering. Journal of Electronic Materials, 53(5), pp. 2410-2420.

[17] Benali, H., Hartiti, B., Lmai, F., Batan, A., Fadili, S., and Thevenin, P., 2024. Synthesis and characterization of Al-doped ZnO thin-films for photovoltaic applications. Materials Today: Proceedings.

[18] Abbas, S. I., Alattar, A. M., and Al-Azawy, A. A., 2024. Enhanced ultraviolet photodetector based on Al-doped ZnO thin films prepared by spray pyrolysis method. Journal of Optics, 53(1), pp. 396-403.

[19] Dejam, L., Kulesza, S., Sabbaghzadeh, J., Ghaderi, A., Solaymani, S., Ţălu, Ş., and hossein Sari, A., 2023. ZnO, Cu-doped ZnO, Al-doped ZnO and Cu-Al doped ZnO thin films: advanced micro-morphology, crystalline structures, and optical properties. Results in Physics, 44, p. 106209.

[20] Ahmed, G., Mohamed, W. S., Hasaneen, M. F., Ali, H. M., and Ibrahim, E. M. M., 2023. Optical, structural, electrical and photocatalytic properties of aluminum doped zinc oxide nanostructures. Optical Materials, 140, p. 113880.

[21] Bouacheria, M. A., Djelloul, A., Adnane, M., Larbah, Y., and Benharrat, L., 2022. Characterization of pure and Al doped ZnO thin films prepared by sol gel method for solar cell applications. Journal of Inorganic and Organometallic Polymers and Materials, 32(7), pp. 2737-2747.

[22] Zhu, M. W., Ma, H. B., Jin, P. H., Jin, Y. N., Jia, N., Chen, H., and Liu, C. Z., 2020. An insight into the low doping efficiency

of Al in sol–gel-derived ZnO: Al films: role of the dopant chemical state. Applied Physics A, 126, pp. 1-9.

[23] Baydogan, N., Ozdurmusoglu, T., Çimenoğlu, H., and Tugrul, A. B., 2013. Refractive index and extinction coefficient of ZnO: Al thin films derived by sol-gel dip coating technique. In Defect and Diffusion Forum (Vol. 334, pp. 290-293). Trans Tech Publications Ltd.

[24] Zhai, C. H., Zhang, R. J., Chen, X., Zheng, Y. X., Wang, S. Y., Liu, J., and Chen, L. Y., 2016. Effects of Al doping on the properties of ZnO thin films deposited by atomic layer deposition. Nanoscale Research Letters, 11, pp. 1-8.

[25] Bedia, A., Bedia, F. Z., Aillerie, M., Maloufi, N., and Benyoucef, B., 2014. Influence of the thickness on optical properties of sprayed ZnO hole-blocking layers dedicated to inverted organic solar cells. Energy Procedia, 50, pp. 603-609.

[26] Ali, Z. H., Bahari, A., and Alarajiy, A. H., 2024. Investigation of the effect of concentration (x) in polyvinyl alcohol (PVA) x/nickel phthalocyanine (NiPc)(1-x) nanocomposites: real & imaginary component of permeability and optical conductivity. Optical Materials, 148, pp 114862.

[27] Shirouzu, K., Ohkusa, T., Hotta, M., et al., 2007. Distribution and solubility limit of Al in Al_2O_3 doped ZnO sintered body. Journal of the Ceramic Society of Japan, 115, pp. 254-258.

[28] Bhattarai, R., Thapa, R. B., Mulmi, D. D., and Ghimire, R. R., 2024. Fabrication of alcohol sensor using undoped and Al-doped ZnO nanostructure film with polymer electrolyte gating. Heliyon, 10(11) pp.1-3.